

Manufacturing Simulation of an Automotive Hood Assembly

Authors:

Chris Galbraith
Metal Forming Analysis Corporation
Centre for Automotive Materials and Manufacturing

Dylan Thomas
Centre for Automotive Materials and Manufacturing
currently with Honda R&D Americas, Inc.

Mark Finn
Alcan International Ltd.

Correspondence:

Chris Galbraith
2582 Highway #2 East
Kingston, Ontario
Canada K7L 4V2

Tel: (613) 547-5395
Fax: (613) 547-5397
e-mail: galb@mfac.com

Keywords:

Manufacturing simulation, spring back, assembly, MPP-DYNA,
stamping, sheet metal forming, functional build.

ABSTRACT

This paper presents the results of applying the finite element method to calculating the spring back of an automotive hood assembly, and its application to the functional build method. The assembly was comprised of six individual panels: an inner panel, an outer panel, a major reinforcement, a latch reinforcement, and two hinge reinforcements.

Finite element simulations were conducted for forming each of the six components. Each component was formed, trimmed, and positioned in car position. The outer panel required several secondary forming operations including a re-meshing, remapping, trim, and flanging operation.

Once in car position, the components were moved so that they just contacted each other, and were "spot welded" together through the application of nodal constraints. Mastic between components was simulated with tied contact. Contact between components was simulated with contact interfaces. Finally, a spring back analysis was conducted.

The models clearly illustrate that it is possible to predict spring back of large automotive assemblies, and that the assembly process yields different final shapes than those obtained from spring back of individual components. With this newly developed tool it is possible to predict whether or not the assembly process can correct out-of-spec components, a key factor in utilizing the functional build method.

INTRODUCTION

A typical automotive body is a complex structure comprised of many sub-assemblies each made of many parts. Often times these parts are sheet metal stampings that must be joined together using spot weld or hemming processes to make the sub-assemblies.

It has been shown by Hammett *et al.*¹ that the final shape of automotive structures is not only affected by residual stresses in the individual stamped parts, but often times by the assembly process itself. Automotive companies typically use a sequential validation process whereby individual stampings are compared to their printed specifications during the die buy-off stage. If the parts do not conform, then the die is reworked until the stamped parts do conform. Often times this effort is wasted as the part would take its desired shape when joined to a stiffer part during the subsequent assembly process. Alternatively, the assembly process itself can distort the shape of individual panels that were produced within specification. The functional build approach recognizes this fact and attempts to take advantage of it: relatively cheap assembly fixtures are used to ensure that during assembly the out of spec components are brought within spec.

While the functional build approach is gaining acceptance in the automotive industry, it is not without its detractors. One of the serious drawbacks is that the functional build approach is a downstream activity. All components to be assembled must first be manufactured before the functional build activity can begin. The investment in tooling for forming each component may be lost if the functional build approach fails to produce an in-spec assembly and the components must be modified so as to bring the assembly into spec. This represents a significant risk to the automotive manufacturers whose risk tolerance decreases dramatically closer to production.

Thomas *et al.*² showed that by modeling the assembly process using the finite element method it is possible to predict the final shape of the automotive assembly, not just the spring back deformation of individual parts. It was also shown that when assembled, the final shape of each part can be considerably different from its shape

when not assembled. The work presented here is an extension of the work conducted by Thomas et al. in that it is applied to a real automotive assembly. The methodologies presented in this paper can be used in conjunction with the functional build approach so as to reduce the risk of relying on a functional build to produce acceptable assemblies. By simulating the forming and the assembly process, it is possible to predict whether or not the assembled component will be within spec. In so doing, it is possible to predict if the functional build approach will be successful, or if the individual components must be modified prior to assembly.

Forming Simulations

The components to be assembled are shown in Figure 1. The components are from a production vehicle and are typical of many hood assemblies constructed with a cruciform inner panel. Although the production vehicle has steel components, they were modeled as if produced from aluminum. For confidentiality reasons, pictures of the inner panel and outer panel are cropped so as to hide some of their identifying features.

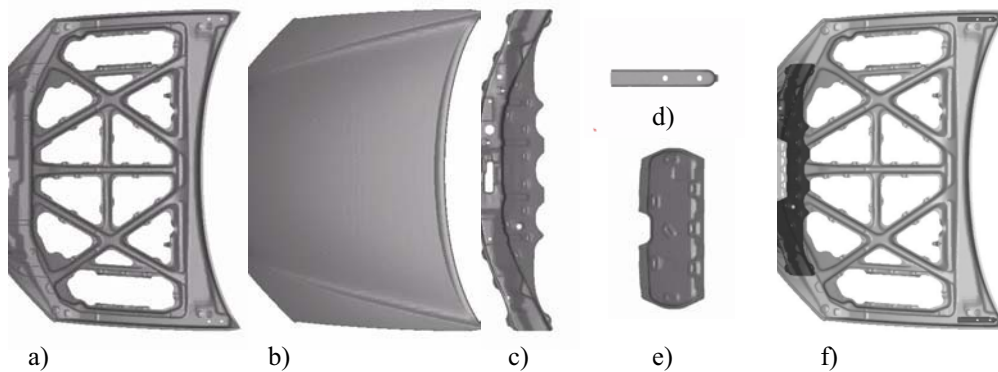


Figure 1 Components to be assembled into the hood assembly. For confidentiality reasons, the inner panel (figure 1a), the outer panel (Figure 1b), and the assembly (Figure 1f) are cropped to prevent identification. a) hood inner b) hood outer c) main reinforcement d) hood hinge reinforcement e) latch reinforcement f) assembly without the outer panel.

The forming simulations were conducted using the MPP version of LS-DYNA³ release 960 running on a Linux Cluster from Medusa Computing Corporation⁴. The explicit dynamic solver was used. Metal forming contact was used to simulate the contact between the work piece (blank) and the tooling. Adaptive remeshing was used so as to increase the number of elements in the blank in areas of high curvature of the tooling and hence reduce discretization errors. Friction between the blank and tooling was modeled with the standard LS-DYNA Coulomb friction model. Mass scaling was not used, but the tool velocities were increased from a natural value of 1 mm/ms to an artificially fast peak of 5 mm/ms, thus reducing the CPU time by a factor of 5. Information about model sizes and run times is provided in Table 1.

Material properties representing the AA6111 aluminum alloy were input to a Barlaet⁵ material model (LS-DYNA Material 36). Stresses, strains, and material thickness values were carried over from forming model to forming model.

Material to be trimmed from the parts was removed through the use of trimming algorithms built into DYNAFORM⁶ pre-processing software. DYNAFORM was also used

to position the formed parts in car position, and to handle the associated stress and strain tensor rotations.

The hood outer panel required a new mesh to be created after the first draw and trim but prior to the pre-hemming operation. This was necessary because the trimming operation created many small elements in the flanges that were unsuitable for further deformation. Surfaces were created that passed through the “as-formed” mesh. These surfaces were then re-meshed. Using the result mapping features of DYNAFORM, the stresses, strains, and thickness distribution were mapped from the original mesh onto the new mesh. The pre-hemming model was cut in half along a symmetry line because of the large number of elements in the new mesh. After running the pre-hemming simulation and coarsening this mesh, the final result for the hood outer was reflected in order to obtain the full model results to be used in the spring back analysis.

Panel	Operation	# of Tooling elements	# of blank elements before	# of blank elements after	CPU Time (hrs)
Hood Inner	1. First Draw	417,737	8,331	374,561	228.4
	2. Trim	n/a	374,561	262,510	n/a
	3. Coarsen	n/a	262,510	122,347	5.0
Hood Outer	1. First Draw	41,070	3,316	37,789	6.3
	2. Trim and map to ½ symmetry	n/a	37,789	50,194	n/a
	3. Prehem	34,549	50,194	129,013	49.1
	4. Coarsen	n/a	129,013	44,554	1.0
	5. Mirror	n/a	44,554	89,108	
	6. Coarsen	n/a	89,108	78,329	0.4
Hinge Reinforcement	1. First Draw	9,566	480	5,112	1.2
	2. Trim	n/a/	5,112	3,074	n/a
	3. Coarsen	n/a	3,074	2,377	0.006
Main Reinforcement	1. First Draw	129,605	2,550	109,338	95.3
	2. Trim	n/a	109,338	40,324	n/a
	3. Coarsen	n/a	40,324	18,787	0.4
Latch Reinforcement	1. First Draw	42,806	2,080	20,941	14.8
	2. Trim	n/a	20,941	6,998	n/a
	3. Coarsen	n/a	6,998	4,427	0.01

Table 1. Model sizes and run times for simulating the forming operations of the individual panels. There are two hinge reinforcements, but model size and timings are identical for each.

Spring Back Calculations

Spring back was calculated for each of the individual panels, and for the assembly. Model run times, memory requirements, and number of steps and iterations are listed in Table 2.

The SMP LS-DYNA implicit solver was used because the MPP version does not currently support contact in implicit analyses. Because plasticity rarely occurs during spring back, the material was modeled as being a linear elastic material. A non-

linear solution is required nonetheless, because of the geometric non-linearities related to large deformation during spring back.

Part Name	# of Elements	Memory (MWords)	# of time steps	# of iterations	CPU Time (hrs:min)
Inner	122,347	230	1	82	10:45
Outer	78,329	137	46	127	10:46
Main Reinforcement	18,787	52	1	9	0:12
Latch Reinforcement	4,427	7	1	9	0:2
Hinge Reinforcement	2,377	9	1	16	0:1.5
Hood Assembly	228,642	514	2	173	76:33

Table 2: Spring back model size and run information. Two hinge reinforcements were included in the assembly.

The default BFGS solver was selected with an iteration limit of unity, meaning that a full-Newton's method was used and that the stiffness matrix was updated at each iteration. Though this approach leads to larger CPU times per iteration, the improved convergence rate decreases the number of iterations and often results in shorter elapsed times.

Boundary conditions were selected that removed 6 rigid body modes (3 rotations and 3 translations). When calculating spring back of the individual components, boundary conditions were selected that mimicked as closely as possible the types of constraints that would be applied to the assembly. Globally, the assembly is constrained such that the nodes around the rear-most hinge bolt on the passenger side are fully constrained not to move in x, y, or z directions. This removes three translational rigid body modes. Constraining the same nodes on the driver side not to move in x- or z-directions removes the z and x rotational degrees of freedom. Finally, a node at the center front of the assembly is constrained not to move in the z-direction, thus removing the y-rotational degree of freedom.

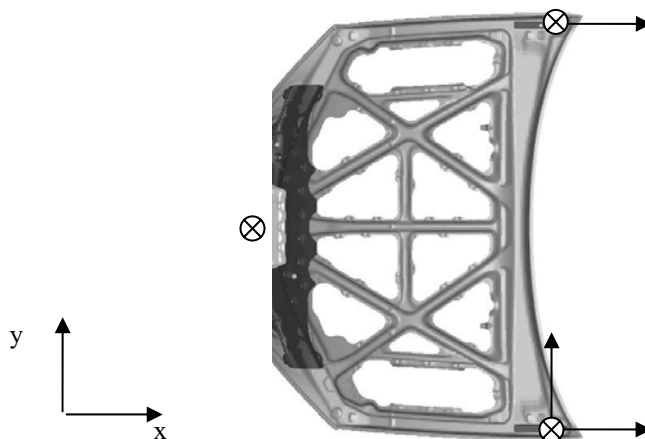


Figure 2. Location of global constraints applied during spring back analysis. The nodes surrounding the passenger side back hinge bolt are fixed in x, y, and z. The drivers side hinge is fixed in x and z. A node at the front of the assembly is fixed in z. When calculating the spring back of the individual components, similar constraints are applied wherever possible.

The z-displacement of the main components during spring back is plotted in Figure 3. Each panel is in car-position for the spring back analysis, so the z-axis is oriented positive upwards (away from the road). The model predicts that the inner panel sags by 2.39 mm along the windscreen. At the same location, the outer panel is high by 5.34 mm. When the outer panel springs back, it develops low spots shown in dark fringes in figure 3b.

Spring Back of the Assembly

The six components were positioned in car position as a starting point for the assembly process. Each of the dynain files from the forming processes were then read into DYNAFORM Version 4.0, as this version is capable of reading in multiple dynain files and automatically reordering the nodes and element numbers to ensure unique numbering when combining input files. A new dynain file was created which contained all six components in roughly the correct position for assembly.

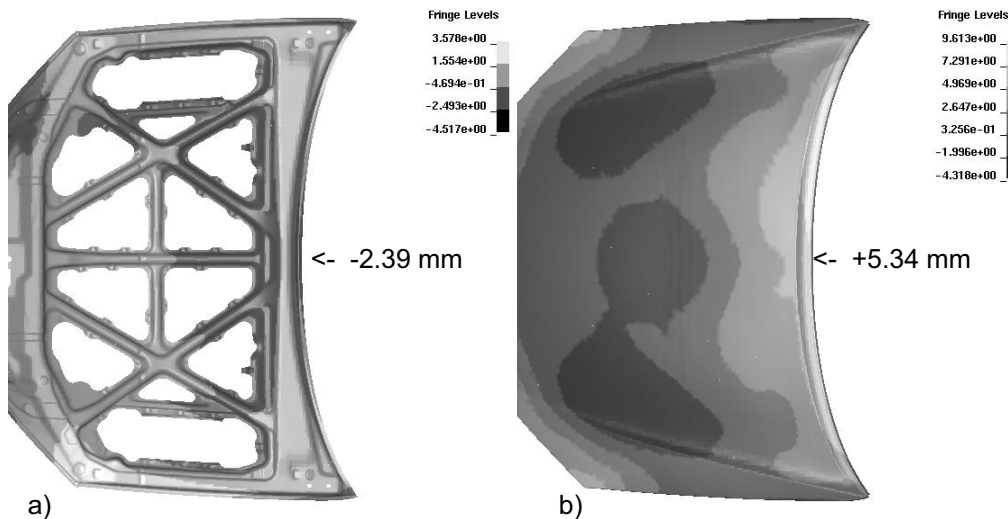


Figure 3. Spring back of Main Components Prior to Assembly. a) hood inner panel b) hood outer panel. Spring back is calculated prior to assembly. Note that the center of the panel at the windscreen rises by 5.34 mm in the outer panel and sags by 2.39 mm on the inner panel.

Final positioning of the parts relative to each other was achieved by modeling contact between all the parts in separate contact interfaces. Table 3 outlines which pairs of parts were checked for contact. LS-DYNA analyses were run to determine at what minimum separation the parts had zero initial penetrations. This was accomplished by setting termination times to zero and sequentially altering the position of each part with the *PART_MOVE keyword. Note that the contact parameters were set so as to include the actual shell thicknesses carried over from the forming models.

With the parts properly positioned, it was possible to impose boundary conditions to mimic the assembly process. In the actual hood assembly, the main reinforcement and latch reinforcement are spot welded together and then spot welded to the inner panel. The hinges are spot welded to the inner panel and a bolt passed between the hinges (not included in this model), the inner panel, and the reinforcement. The outer panel is attached to the inner by hemming along the windscreen and the sides, and by spot welding along the front of the panel.

	Inner	Outer	Main	Latch	Hinges
Inner	No	Yes	Yes	No	Yes
Outer	Yes	No	Yes	Yes	No
Main	Yes	Yes	No	Yes	No
Latch	No	Yes	Yes	No	No
Hinge	Yes	No	No	No	No

Table 3. Contact interfaces were applied between the parts according to the entries in this table.

Each of these assembly methods is simulated in the models except for the hemming operation. Instead, spot welds are applied between the inner and the outer along the flanges.

The mastic was modeled with a tied contact between the inner and outer panel. The *CONTACT_TIED_OFFSET parameters were selected such that any gaps of less than 5 mm between the inner and outer panel would be filled with mastic, tying the inner to the outer.

The spring back model for the assembly contained six parts, nine different contact algorithms, and 228,642 elements. With such a large model, the memory requirements were substantial. The model required an allocation of 514 MWords (4.11 GBytes) of RAM in order to perform the in-core solution using solver 6 – the BCSLIB-EXT direct sparse double precision solver. The double precision solver was required because the short integers in the single precision code could not store integers large enough to hold the memory locations for the entire stiffness matrix. Although the double precision code has the advantage of improved convergence due to reduced round-off error during Gaussian elimination, it does require twice as much memory as the single precision code.

Convergence of the full Newton's method occurred in 2 time steps consisting of a total of 173 iterations. The artificial stabilization approach was taken for the multi-step simulation.

The z-deflection of the assembly is shown in Figure 4. In comparison to the plots in Figure 3, it can be seen that the assembly process dramatically alters the deflections of the individual components. The three low spots seen in Figure 3b have been replaced by a single, smaller low spot in Figure 4b.

The spring back of the assembly is less than that of the original unassembled components. This illustrates the possibilities inherent in the functional build approach. The stiffness of the inner panel is used to keep the outer panel closer to the specification. The use of low-cost assembly fixtures could be used to get the part within spec. Rather than spending time and money minimizing spring back of individual panels, the work can be focused on the assembly process.

Summary and Conclusions

With recent advances in LS-DYNA, it is now possible to simulate an assembly process for a component comprised of multiple sub-components. The implicit solver has become more robust and is now capable of handling significantly larger models than in the past. Extension of the MPP code to include implicit contact is required before that code can be used for doing implicit spring back calculations, but once this ongoing work is completed, it should allow even larger assemblies to be studied. In this

way, the functional build approach can be more easily implemented with less risk to the automotive manufacturer.

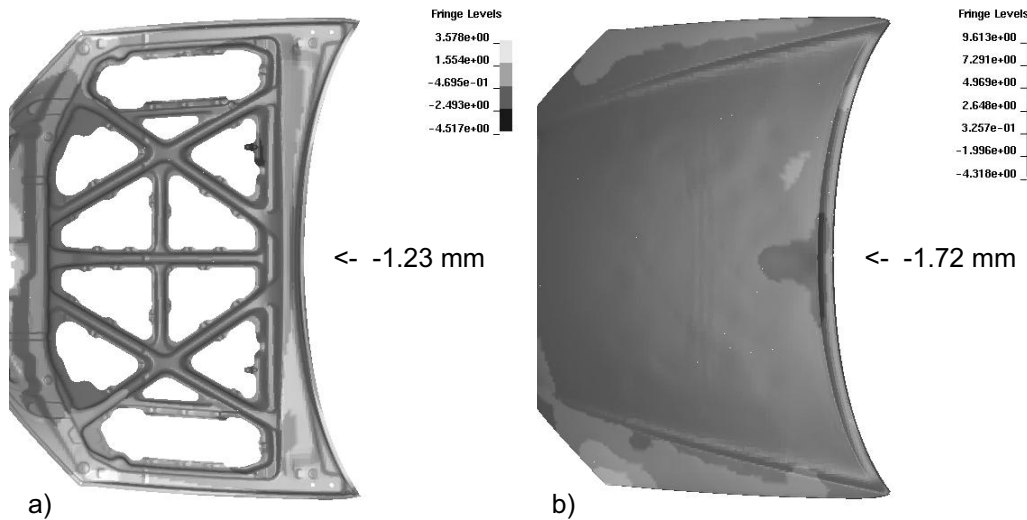


Figure 4. Spring back of the inner panel and outer panel after assembly. Note the differences when compared to Figure 3. The three low spots seen in Figure 3b for the outer are replaced by one smaller low spot along the wind screen.

References

1. PATRICK C. HAMMETT, KARL D. MAJESKE, JAY S. BARON. (1998) "Functional build: Integrating automotive body-design & process-development". In Proceedings of the Annual Reliability and Maintainability Symposium, pages 1-19. IEEE, 1998
2. THOMAS, D.N., GALBRAITH, P.C., BULL, M.J., FINN, M.J. (2002) "Prediction of Springback and Final Shape in Stamped Automotive Assemblies: Comparison of Finite Element Predictions and Experiments". In Proceedings of IBEC 2002. 02IBECC-11.
3. HALLQUIST, J.O. (2001) LS-DYNA Keyword User's Manual Version 960, Volumes 1 & 2. Livermore Software Technology Corporation.
4. Medusa Computing Corporation. 2582 Highway #2 East, Kingston, Ontario, Canada. K7L 4V1
5. DYNAFORM User's Manual. (2001) Engineering Technology Associates, Inc. 1133 E. Maple Road, Suite 200 Troy MI 48083, USA.
6. BARLAT, F., LIAN, J. (1989) "Plastic behavior and stretchability of sheet metals. Part 1: A yield function for orthotropic sheets under plane stress conditions". International Journal of Plasticity, 5:51-66.